

## Optimal Sampling of the Rotation Function

BY EATON E. LATTMAN

Thomas C. Jenkins Department of Biophysics, Johns Hopkins University, Baltimore, Maryland 21218, U.S.A.

(Received 19 July 1971)

A method of sampling the rotation function is presented which requires fewer sample points, produces undistorted maps whose coordinates are locally orthogonal, and associates equal volumes with all sample points.

### Introduction

During the past decade or so, a number of applications of the rotation function of Rossmann & Blow (1962) and of other related methods (Huber, 1965; Nordman & Nakatsu, 1963; Tollin & Cochran, 1964; Lattman & Love, 1969) have been reported. These methods have in common the calculation of an index of agreement or overlap between two three-dimensional structures, as a function of their relative orientation. A typical example is the function:

$$R(\mathbf{C}) = \sum_{\mathbf{h}} F^2(\tilde{\mathbf{C}}\mathbf{h})I(\mathbf{h}), \quad (1)$$

used by Lattman & Love to search for the orientation at which the diffraction pattern  $F^2$  from an isolated molecule is in best coincidence with the pattern  $I(\mathbf{h})$  from a crystal. The matrix  $\mathbf{C}$  is a rotation operator which varies the relative orientation of the two patterns,  $R$  is the rotation function, and the summation is taken over the reciprocal lattice vectors  $\mathbf{h}$  of the crystal.

The matrix  $\mathbf{C}$  is usually expressed in one of two systems of angular variables. The Eulerian angles  $\theta_1, \theta_2, \theta_3$  ( $\Theta$ ), well known in classical mechanics, are described by Goldstein (1959), and by Rossmann & Blow. Tollin, Main & Rossmann (1966) have shown that the symmetry of the rotation function appears in a particular simple way through the use of these angles.

The second angular system makes use of the theorem that any rotation can be accomplished by an appropriate spin about a properly chosen axis. The spherical polar angles,  $\varphi$  and  $\psi$ , specify the longitude and colatitude of this axis, and the azimuthal angle,  $\chi$ , specifies the spin about it. This system is labor-saving whenever either the direction or order of a non-crystallographic axis of symmetry can be anticipated.

Lattman & Love, among others, have evaluated  $R$  on a grid having equal, constant steps in  $\theta_1, \theta_2, \theta_3$ . This grid produces uneven and inefficient sampling which is costly in computer time. Since rotation function calculations are extremely expensive, this difficulty is not trivial. In addition, the apparent breadth and separation of peaks are strongly dependent on their location. Plots of the rotation function are consequently inconvenient to deal with. Finally, it is well known that

the integrated density beneath a peak in a correlation function is often a better measure of its importance than its height. Since points in this grid do not all have equal volumes associated with them, it is difficult to calculate such integrated densities.

For these reasons, the above-mentioned grid in  $\Theta$  is unsatisfactory. Comparable difficulties have also arisen when using analogous grids in the angles  $\varphi, \psi, \chi$  ( $\Phi$ ). Described herein is a procedure for the efficient selection of sample points using either angular system. The procedure decreases computation time and distortion, and associates approximately equal volumes with the sample points.

### Methods

Functions defined in a three-dimensional, Euclidian space, such as electron density functions, are customarily evaluated at the nodes of a sampling lattice whose base vectors are roughly equal in length and roughly orthogonal. The volumes associated with all sample points are equal. To extend these notions to the angular space explored in equation (1), first an intuitively pleasing definition of the 'distance' between two orientations is adopted which then is shown to lead automatically to orthogonality of small increments in the angular variables.

Since any two orientations of a body are related by a single rotation  $\chi$ , it seems appropriate to define the 'distance' between these orientations as the magnitude of the spin  $\chi$  which transforms one into the other. More formally, if  $O_1$  and  $O_2$  are two orientations which are related to a standard orientation  $O$  by the operators  $\mathbf{C}(\omega_1)$  and  $\mathbf{C}(\omega_2)$ , then the distance between  $O_1$  and  $O_2$  is defined as the magnitude of the angle  $\chi_d$  which satisfies the equation:

$$\mathbf{C}(\omega_2) = \mathbf{P}(\varphi, \psi, \chi_d)\mathbf{C}(\omega_1). \quad (2)$$

Here,  $\omega_1$  and  $\omega_2$  are angular triples, and the matrix  $\mathbf{P}$  transforms  $O_1$  into  $O_2$ .

Adjacent sample points in the rotation function represent orientations which differ by small changes in the defining angular variables. It is therefore desirable to calculate the distance between such nearby orientations. Eulerian angles are considered first. It happens that the results are most useful if a linear recombina-

tion of the conventional Eulerian angles is defined. We use the quasi-orthogonal Eulerian angles  $\theta_+$ ,  $\theta_2$ ,  $\theta_-$  ( $\theta_{\pm}$ ) where

$$\theta_+ = \theta_1 + \theta_3, \quad \theta_- = \theta_1 - \theta_3. \quad (3)$$

These variables have a certain physical plausibility. When  $\theta_2$  is near 0 or  $\pi$ , the rotations  $\theta_1$  and  $\theta_3$  are strongly coupled. Here, on the other hand, when  $\theta_2=0$ , changes in  $\theta_-$  have no effect on orientation; all dependence appears in  $\theta_+$ . Similarly, when  $\theta_2=\pi$  all the dependence appears in  $\theta_-$  and changes in  $\theta_+$  have no effect.

To solve equation (2) for  $\chi_a$ , both sides are multiplied by  $\tilde{\mathbf{C}}(\omega_1)$ , the transpose of  $\mathbf{C}$ , to yield:

$$\mathbf{P}(\varphi, \psi, \chi_a) = \mathbf{C}(\theta_+, \theta_2, \theta_-) \cdot \tilde{\mathbf{C}}(\theta_+ + \Delta\theta_+, \theta_2 + \Delta\theta_2, \theta_- + \Delta\theta_-), \quad (4)$$

where the quasi-orthogonal angles and the small increments therein have been specifically inserted. Since equation (4) is a matrix equation, it is true element by element. Equating the sum of the diagonal elements on both sides of equation (4):

$$\sum_{i=1}^3 P_{ii} = 1 + 2 \cos(\chi_a) = \sum_{i,j=1}^3 C_{ij}(\theta_{\pm}) \cdot C_{ij}(\theta_{\pm} + \Delta\theta_{\pm}) \quad (5)$$

where  $P_{ij}$  and  $C_{ij}$ , the elements of  $\mathbf{P}$  and  $\mathbf{C}$ , are given explicitly in Table 1. Inserting these quantities into equation (5) and making use of expansions of the form:

$$\begin{aligned} \frac{\sin(\omega + \Delta\omega)}{\cos(\omega + \Delta\omega)} &= \frac{\sin(\omega) \pm \Delta\omega \cdot \cos(\omega)}{\cos(\omega) \mp \frac{\Delta\omega^2}{2} \cdot \frac{\sin(\omega)}{\cos(\omega)}}, \end{aligned} \quad (6)$$

it follows that

$$\chi_a^2 = \Delta\theta_+^2 \cdot \cos^2(\theta_2/2) + \Delta\theta_2^2 + \Delta\theta_-^2 \cdot \sin^2(\theta_2/2). \quad (7)$$

Higher-order terms have been ignored.

We see that  $\chi_a^2$ , the square of the distance between

nearby orientations, is given by a sum of terms quadratic in the angular increments. This Pythagorean form shows that the quasi-orthogonal Eulerian angles are, in fact, locally orthogonal. Use of the conventional Eulerian angles in equations (4) to (7) would have generated a term containing  $\Delta\theta_1\Delta\theta_3$  in (7), demonstrating their nonorthogonality.

When  $R$  is calculated as a function of  $\theta_{\pm}$ , the procedure for uniform sampling is clear. Angular steps are taken that keep constant the quantities  $\Delta\theta_+ \cdot \cos(\theta_2/2)$ ,  $\Delta\theta_2$ ,  $\Delta\theta_- \cdot \sin(\theta_2/2)$ . If sections of constant  $\theta_2$  are calculated, the steps in  $\theta_+$  and  $\theta_-$  do not vary within a section. The steps between sections are also constant.

Fig. 1(a) and (b) display the same rotation function section calculated using conventional and quasi-orthogonal Eulerian angles. Because of the small value of  $\theta_2$ , the peak in the conventional map is greatly elongated in one direction. When the same peak is plotted using the methods just described, it has a natural and fairly symmetrical shape.

Tollin *et al.* (1966) have given an elegant discussion of the symmetry of the rotation function, and they describe what range of  $\theta$  must be explored under various circumstances. The corresponding range of  $\theta_{\pm}$  is easily derived. For example, when the functions being compared have no symmetry, the volume bounded by  $-\pi \leq \theta_1 < \pi$ ,  $0 \leq \theta_2 < \pi$ ,  $-\pi \leq \theta_3 < \pi$  must be explored. The corresponding region for  $\theta_+$  and  $\theta_-$  is diamond shaped, and is shown in Fig. 2(a). For  $\theta_2$  there is no change. Simultaneous translations of  $\pm 2\pi$  in  $\theta_+$  and  $\theta_-$ , identity operations, shift the two cross-hatched triangles in Fig. 2(a) to the positions shown in Fig. 2(b), providing a convenient rectangular range in the  $\theta_+, \theta_-$  plane. Analogous regions can be derived when there is symmetry in the rotation function.

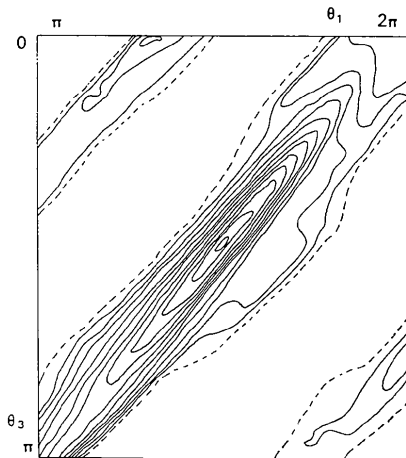
For a given angular step  $D$ , a conventionally sampled map requires  $(2\pi/D)^2$  grid points to explore the region in Fig. 2(a). For orthogonal sampling, this number is a function of  $\theta_2$  and is given by  $(4\pi/D) \cdot [\cos(\theta_2/2)] \times (2\pi/D) \cdot [\sin(\theta_2/2)] = (2\pi/D)^2 \cdot \sin(\theta_2)$ . The mean value of  $\sin(\theta_2)$  is  $2/\pi$ , and so an orthogonally sampled map

Table 1. (a) Matrix  $\mathbf{C}$  in terms of Eulerian angles  $\theta_1, \theta_2, \theta_3$  and (b) matrix  $\mathbf{C}$  in terms of rotation angle  $\chi$  and spherical polar coordinates  $\psi, \varphi$

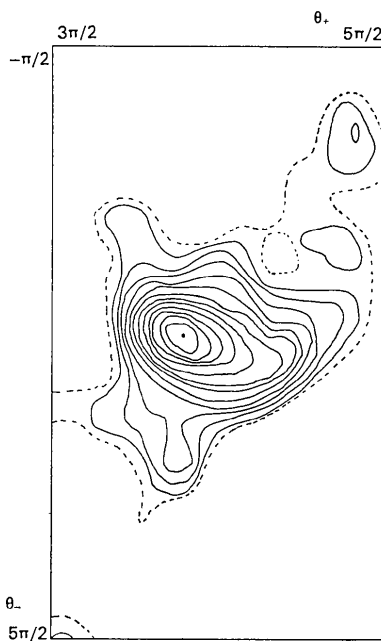
(a)		
$-\sin \theta_1 \cos \theta_2 \sin \theta_3$ $+\cos \theta_1 \cos \theta_3$	$\cos \theta_1 \cos \theta_2 \sin \theta_3$ $+\sin \theta_1 \cos \theta_3$	$\sin \theta_2 \sin \theta_3$
$-\sin \theta_1 \cos \theta_2 \cos \theta_3$ $-\cos \theta_1 \sin \theta_3$	$\cos \theta_1 \cos \theta_2 \cos \theta_3$ $-\sin \theta_1 \sin \theta_3$	$\sin \theta_2 \cos \theta_3$
$\sin \theta_1 \sin \theta_2$	$-\cos \theta_1 \sin \theta_2$	$\cos \theta_2$
(b)		
$\cos \chi$ $+\sin^2 \psi \cos^2 \varphi (1 - \cos \chi)$	$\sin \psi \cos \psi \sin \varphi (1 - \cos \chi)$ $-\sin \psi \sin \varphi \sin \chi$	$-\sin^2 \psi \cos \varphi \sin \varphi (1 - \cos \chi)$ $+\cos \psi \sin \chi$
$\sin \psi \cos \psi \cos \varphi (1 - \cos \chi)$ $+\sin \psi \sin \varphi \sin \chi$	$\cos \psi$ $+\cos^2 \psi (1 - \cos \chi)$	$-\sin \psi \cos \psi \sin \varphi (1 - \cos \chi)$ $-\sin \psi \cos \varphi \sin \chi$
$-\sin^2 \psi \sin \varphi \cos \varphi (1 - \cos \chi)$ $-\cos \psi \sin \chi$	$-\sin \psi \cos \psi \sin \varphi (1 - \cos \chi)$ $+\sin \psi \cos \varphi \sin \chi$	$\cos \chi$ $+\sin^2 \psi \sin^2 \varphi (1 - \cos \chi)$

requires only  $2/\pi$  times as many sample points as a conventionally sampled one.

Because the scales along the  $\theta_+$  and  $\theta_-$  axes change as a function of  $\theta_2$ , the range of  $\theta_{\pm}$ , as it appears on the printed page, has a rather peculiar shape. It looks roughly like a pair of wedges placed base-to-base in the plane  $\theta_2 = \pi/2$ , with the edges forming a single row in the plane  $\theta_2 = 0$  and a single column in the plane  $\theta_2 = \pi$ .

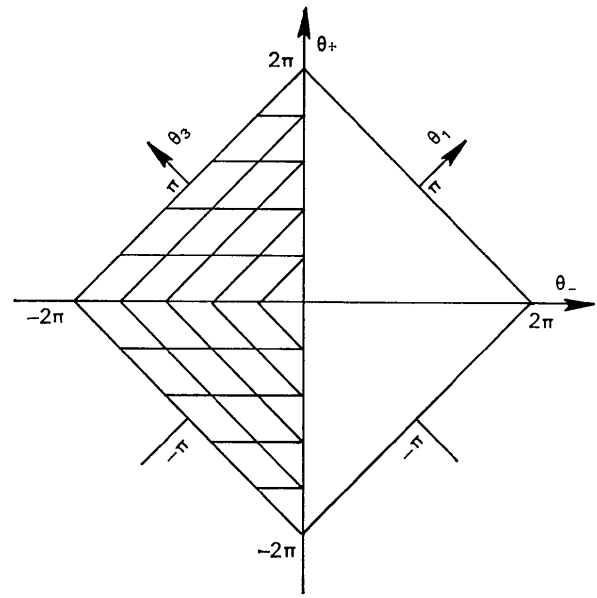


(a)

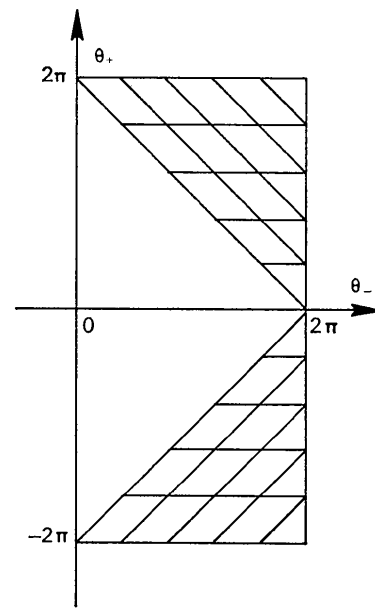


(b)

Fig. 1. (a) A section at  $\theta_2 = 15^\circ$  from the rotation function, comparing the diffraction patterns from an isolated molecule and crystal of sperm whale myoglobin. The coordinates  $\theta_1$  and  $\theta_3$  have been sampled in steps of  $5^\circ$ . The peak is extremely extended in one direction and difficult to interpret. (b) The same section calculated with respect to  $\theta_+$  and  $\theta_-$ . Steps of  $5^\circ$  in  $\theta_+$  and  $35^\circ$  in  $\theta_-$  were taken. The peak is now much more symmetrically shaped, and only about one seventh as many points were required.



(a)



(b)

Fig. 2. (a) A square asymmetric unit in the  $\theta_1\theta_3$  plane. With respect to the  $\theta_+$  and  $\theta_-$  axes, also shown, it is inconveniently oriented for plotting. (b) The hatched triangles in (a) have been moved by identity translations of  $\pm 2\pi$  in  $\theta_1$  and  $\theta_3$  to yield a rectangular area better suited to the  $\theta_+$  and  $\theta_-$  axes.

Orthogonal sampling also ensures that equal volumes are associated with each sample point. The volume of the parallelepiped with edges  $\Delta\theta_+$ ,  $\Delta\theta_2$ ,  $\Delta\theta_-$  is:

$$V = \sin(\theta_2/2) \cos(\theta_2/2) \Delta\theta_+ \Delta\theta_2 \Delta\theta_- \quad (8)$$

$$= \frac{1}{2} \sin(\theta_2) \Delta\theta_+ \Delta\theta_2 \Delta\theta_-$$

a quantity which is constant throughout the map.

The situation for the angles  $\varphi, \psi, \chi$  is dealt with very briefly. Expressing  $\mathbf{C}$  in equation (4) in terms of these angles, the distance  $\chi_a$  as a function of the angles and their increments can be calculated, such that

$$\chi_a^2 = \Delta\chi^2 + 4 \sin^2(\chi/2)\Delta\psi^2 + 4 \sin^2(\chi/2) \sin^2(\psi)\Delta\varphi^2. \quad (9)$$

These variables are, therefore, also locally orthogonal. Maps computed as functions of  $\boldsymbol{\varphi}$  are usually plotted on sections of constant  $\chi$ , with  $\psi$  and  $\varphi$  being represented on the surface of a sphere. In this way, equal areas on the sphere correspond to equal areas in  $\boldsymbol{\varphi}$  space. There is, however, a factor  $4 \sin^2(\chi/2)$  weighting the different levels [see equation (9)]. When  $\chi$  is small, large areas and lengths on the sphere correspond to much smaller quantities in  $\boldsymbol{\varphi}$  space. Thus, peaks that appear widely separated may actually be only a small distance apart. Note also that the local orthogonality of  $\varphi$  and  $\psi$  is preserved on the sphere, so that the selection of sample points is fairly straightforward.

There have been two previous attempts to achieve satisfactory sampling of the rotation function. Tollin & Cochran (1964) searched a Patterson function with a featureless disc. This rotational search, therefore, consists of placing the disc normal at representative points on the unit sphere, and the distance between orientations is the great-circle distance between the positions of the tip of the normal vector. For small distances this works out to be:

$$\chi_a^2 = \sin^2(\psi)\Delta\varphi^2 + \Delta\psi^2. \quad (10)$$

Tollin & Cochran chose, in an *ad hoc* way, a sampling technique which corresponds to the distance equation

$$\chi_a^2 = (2\psi/\pi)^2\Delta\varphi^2 + \Delta\psi^2. \quad (11)$$

For  $\psi$  near  $\pi/2$ , equations (10) and (11) are nearly identical. For  $\psi$  near 0, Tollin & Cochran choose steps in  $\varphi$  which are too large by a factor  $\pi/2$ . There are few

sample points in this range, however, so that their scheme is a very good one.

In a paper brought to the author's attention after this work was completed, Burdina (1971) has investigated many of the problems discussed herein. Choosing a metric like that defined in equation (2) he derives an equation like equation (8), in terms of conventional Eulerian angles. The sampling scheme he presents, however, does not have the distortion-free character of the technique presented here. In addition, Burdina discusses some interesting problems in the symmetry of the rotation function.

### Conclusions

This paper has presented a method for sampling the rotation function which reduces computation time, yields undistorted maps, and associates equal volumes of angle space with each sample point.

I should like to thank Drs Warner Love and Wayne Hendrickson for helpful discussions. This work has been supported by grant AM02528 from the USPHS, and by a grant for computing from the Johns Hopkins University.

### References

- BURDINA, V. I. (1971). *Sov. Phys. Cryst.* **15**, 545.  
 GOLDSTEIN, H. (1959). *Classical Mechanics*, p. 93. Reading: Addison-Wesley.  
 HUBER, R. (1965). *Acta Cryst.* **19**, 353.  
 LATTMAN, E. E. & LOVE, W. E. (1969). *Acta Cryst.* **1326**, 1854.  
 NORDMAN, C. E. & NAKATSU, K. (1963). *J. Amer. Chem. Soc.* **85**, 353.  
 ROSSMANN, M. G. & BLOW, D. M. (1962). *Acta Cryst.* **15**, 24.  
 TOLLIN, P. & COCHRAN, W. (1964). *Acta Cryst.* **17**, 1322.  
 TOLLIN, P., MAIN, P. & ROSSMANN, M. G. (1966). *Acta Cryst.* **20**, 404.